

A comparative study by mechanical activation and conventional processes of $\text{BaTi}_{0.95}\text{W}_{0.05}\text{O}_3$ ferroelectric ceramic

Anushka Tyagi¹, Shruti Chaudhary¹, Sheela Devi², and Shilpi Jindal^{1*}

¹ Department of Physics, Chandigarh University, 140413, Gharuan, Mohali, Punjab, India

² Department of Applied Sciences, MSIT, C-4,110058, Janakpuri, New Delhi, India

Abstract. $\text{BaTi}_{0.95}\text{W}_{0.05}\text{O}_3$ is synthesized by both mechanical activation process and conventional solid-state reaction technique for comparative study. The prepared sample is characterized by XRD and SEM. There is proper formation of perovskite structure in BTW from both of the methods confirmed by XRD. Scanning electron microscopy (SEM) depicts that the micro-grains obtained by the mechanical activation method had comparatively fine structure compared to that of the conventional solid-state process. The mechanically activated samples display enhanced electrical properties showing a high value of the dielectric constant and a low value of the dielectric loss. The remnant polarization (Pr) value and d_{33} values were also high in samples synthesized by the mechanical method.

1 Introduction

Barium titanate is among the most commonly used ferroelectric material with a perovskite structure. Perovskite structure is an ABO_3 type structure, where A is 12-fold coordination concerning oxygen and B is coordinated octahedrally to oxygen atoms. The first-ever perovskite found was CaTiO_3 with space group Pm-3m. It is widely used because of its high dielectric constant and low value of dielectric loss [1]. BT is reported by many researchers via different techniques such as the solid-state method, sol-gel process, hydrothermal method, mechanical activation process, and many more. Barium titanate is one of the most frequently used lead-free ferroelectric and piezoelectric materials [2]. Although, BT has low ferroelectricity and piezoelectricity as compared to lead-based materials but also shows some similar properties to that of lead-containing perovskite material which makes it the area of interest for researchers. BT shows cubic structure above T_c which is around 130 °C whereas, below T_c , the structure is slightly distorted towards a tetragonal structure. Also, other transformations take place at temperature ranges close to 0°C and -80°C which gets transformed from firstly to orthorhombic with polar axis parallel to a face diagonal and finally transformed to rhombohedral structure with polar axis along a body diagonal respectively. The transformation which also shows the corresponding changes in lattice parameters and

*Corresponding author: shilpi.uis@cumail.in

spontaneous polarization. BT has attained great industrial importance and has many applications such as capacitors and multilayer capacitors (MLCs), sensors, and piezoelectric or pyroelectric devices [3-5]. Recently, many researchers were using this high-energy ball milling technique for the synthesis of nanocrystalline ceramics. In this method high mechanical energy is activated by milling the sample in between the metal balls to initiate the solid-state reaction of the oxides [6-9]. This process does not require a calcination part which consumes very high energy, which makes this preparation technique simpler than that of the conventional method. This led the authors to synthesize $\text{BaTi}_{0.95}\text{W}_{0.05}\text{O}_3$ by the novel mechanical activation process. The main purpose of preparing the sample by both methods is to compare its structural, dielectric, and ferroelectric properties so that they can find better ways of using it in many applications.

Sheela et al. in 2008 and 2009 explained when tungsten is substituted for titanium in barium titanate, a single-phase perovskite structure is formed and the Curie temperature decreases from 110°C to 85°C. Dielectric investigations show that these compounds have a diffuse ferro-paraelectric phase transition with increasing diffusivities. Both the dielectric constant and the loss are found to decrease with frequency. All of the samples exhibit PTCR behavior. [10-12] $\text{BaW}_{0.05}\text{Ti}_{0.95}\text{O}_3$ (BWT) was made by ball milling for different times (10, 20, and 30 hours) by Shristi et al. The microstructural, dielectric, and impedance research are discussed in this study. The creation of a single phased tetragonal structure and a perovskite structure is revealed by microstructural studies utilizing XRD data. The partial replacement of W (at the B site) considerably improved the dielectric characteristics of BT nanoceramics, demonstrating the diffuse phase transition at 80°C. Dielectric loss increases with increasing temperature. The charge carrier mobility increases, resulting in enhanced polarization and considerable dielectric loss. Furthermore, when compared to the un-milled BWT ceramic sample, 30 hours milled had improved dielectric properties with a higher dielectric constant and lower loss. [13]

In this paper we discussed about the effect on structural and dielectric properties of tungsten doped Barium titanate synthesized by two different methods i.e. mechanical activation and the conventional solid-state method. Microstructural properties were carried out by XRD, SEM and TEM characterization techniques whereas dielectric studies were carried out by LCR meter and ferroelectric properties were carried out by P-E loops.

2 Experimental

2.1 Materials and Methods

Mechanical activation and the traditional solid-state technique were used to prepare the material with a precise concentration of $\text{BaTi}_{0.95}\text{W}_{0.05}\text{O}_3$. The oxides and carbonates (BaCO_3 , TiO_2 , and WO_3) from Aldrich, all of 99.9% purity, were taken in accordance with their stoichiometric ratio as starting material for the synthesis of $\text{BaTi}_{0.95}\text{W}_{0.05}\text{O}_3$. This stoichiometric ratio of the specified components was ground for 30 hours at a speed of about 400 rpm in a high-energy ball mill (Retsch-PM 100) for the mechanical activation procedure. With an 8:1 ball-to-powder weight ratio, 10 mm zirconium oxide balls were milled in a toluene medium within a zirconium oxide vial. The pellets were kept for sintering at 1250°C for 2 hours. Talking about the conventional solid-state method the additional step is calcination which is done after grinding the starting materials for 4-6 hours. The calcination is done in a muffle furnace at a higher temperature and afterward the same process sintering and pelletization just like the activation method. At last, characterization is done such as XRD, SEM, TEM, and dielectric measurements are also observed.

2.2 Characterization Techniques

Using a Bruker diffractometer (model D8 Advance) with $\text{CuK}\alpha$ radiation ($\lambda = 1.5405 \text{ \AA}$) and a scanning rate of $1^\circ/\text{min}$, the X-ray patterns of the sintered pellets were recorded. The powder's particle size can be determined by Transmission Electron Microscopy (TEM) characterisation (Technia G2 F 30S TWIN). SEM, or the Hitachi-S3700 Scanning Electron Microscope, operates at 15 kV and provides information about the granular morphology of the materials. After sintering, the resulting pellets were polished and delicately silver pasted on both sides, then cured for 15 minutes at 300 oC. A precision LCR metre (Agilent 4284A) running at an oscillation amplitude of 1 V was used to test the dielectric. Using a P–E loop tracer, the polarization–electric field (P–E) hysteresis loops were captured using Sawyer–Tower circuit. The samples were poled at 17 kV/cm at an elevated temperature for 8 hours in silicon oil. Piezoelectric co-efficient, d_{33} values, were measured using a piezometer system (PiezoTest PM300).

3 Results and Discussion

3.1 Structural and microstructural analysis

XRD patterns of both methods are shown in Figure 1. The pattern revealed the formation of a single-phase from both the preparation techniques with no impurity peaks. The $\text{BaTi}_{0.95}\text{W}_{0.05}\text{O}_3$ has tetragonal perovskite structure with hkl values $\langle 100 \rangle$, $\langle 101 \rangle$, $\langle 111 \rangle$, $\langle 200 \rangle$, $\langle 201 \rangle$, $\langle 211 \rangle$ confirmed by the diffractograms. Lattice parameters and cell volume were calculated for both methods. All the calculated parameters were reported in Table 1. It is observed that the values of the calculated parameter come out to be almost the same but the d_{33} values differ.

The crystallite size of the specimen is calculated using selected intense peaks at different Bragg angles using Scherer's formula [13],

$$D = K\lambda/\beta\text{Cos}\theta$$

Where, $K = 0.9$, β is the FWHM of the peak and θ is the diffraction angle. To avoid strain broadening, a peak in the lower angle region is chosen.

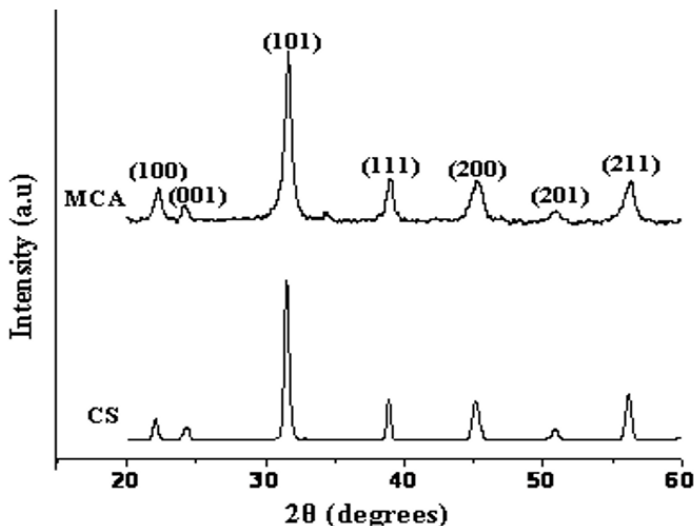


Fig. 1. XRD pattern of $\text{BaTi}_{0.95}\text{W}_{0.05}\text{O}_3$ by mechanical activation process (MCA) and conventional solid-state method (CS)

Table 1. Lattice parameters of BTW

Parameters	Conventional	MCA
Sintering temperature (°C)	1250	1250
c(Å)	4.025	4.014
a (Å)	3.996	3.9915
Volume (Å) ³	64.271	64.037
c/a	1.0072	1.0069
d ₃₃ (pC/N ⁻¹)	102.5	257

Figure 2 shows the SEM images of the W doped Barium titanate. The characteristic images of SEM prepared from both the methods are shown in 2(a) and 2(b) respectively. The grain size of BTW for both methods is 2µm and it has been observed that the variation in the morphology of the grains activated by the dopant would also lead to the favored orientation [14]. Fig. 2 (a) and (b) show SEM images of all the compositions above said composition prepared at varying milling duration. It is visible from the images that a reduction in grain size is observed at higher milling temperature which is responsible for the agglomeration of the particles. The synthesized particles possessed almost spherical morphology with uniform distributed particle size. The linear intercept method was used to determine the grain size which is ~ 0.3-0.2 µm. TEM and SAED images of the sample milled for 30 hours; were also presented in Fig. 3 which showed the size of particles between 20 nm to 50 nm. The successful fabrication of nanoparticles is visible via diffraction rings made up of diffraction spots in electron diffraction graph. The results obtained were by XRD result for determining crystallite size.

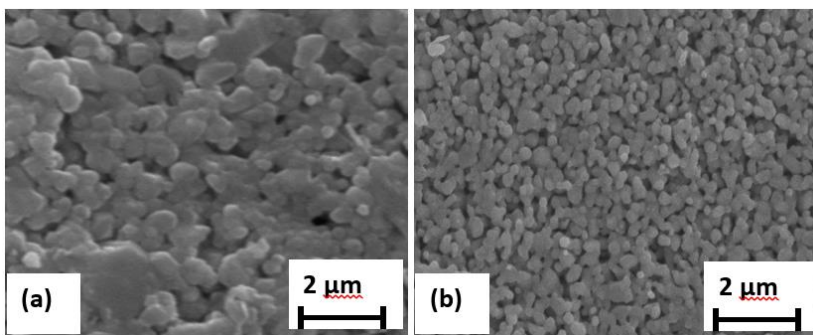


Fig. 2. SEM images of $\text{BaTi}_{0.95}\text{W}_{0.05}\text{O}_3$

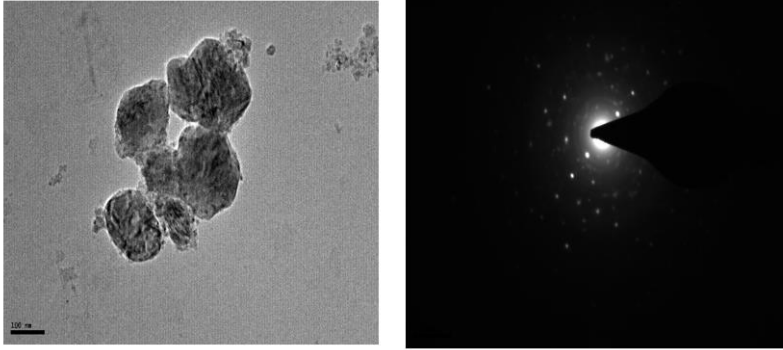


Fig. 3. TEM and SAED images of $\text{BaTi}_{0.95}\text{W}_{0.05}\text{O}_3$

3.2 Dielectric Analysis

Figure 4 shows the effect of temperature (from the range of 20° to 160°C) on dielectric constant at different frequencies which gives a better knowledge of the associated polarization mechanism and significant to knowing about the ferroelectric-based applications of the prepared samples. Previous study reported that the standard dielectric constant of pure Barium Titanate is between 120°C and 130°C. The dielectric study reveals that the Curie temperature (T_c) is around 70°C-80°C due to tungsten doping in Barium titanate for both methods. Figure 5 represents the variation in dielectric loss at varying temperatures for both methods. The loss tangent of the sample is observed negligible at lower temperature ranges up to 100°C then there is a significant increase at higher temperature ranges [14-16]. The only difference in the loss tangent plots is that there is a very sharp increase in loss tangent for the conventional solid-state method and case of the activation method, at low frequency, the loss tangent increases after 100°C but at the higher frequency, it does not increase as much. The tangent loss is the ratio of the imaginary part to the real part of permittivity. It gives the value of energy dissipated in a system, which varies under the imaginary part of the dielectric constant. Owing to dipoles towards polarization, losses were reduced at higher frequencies [17-20].

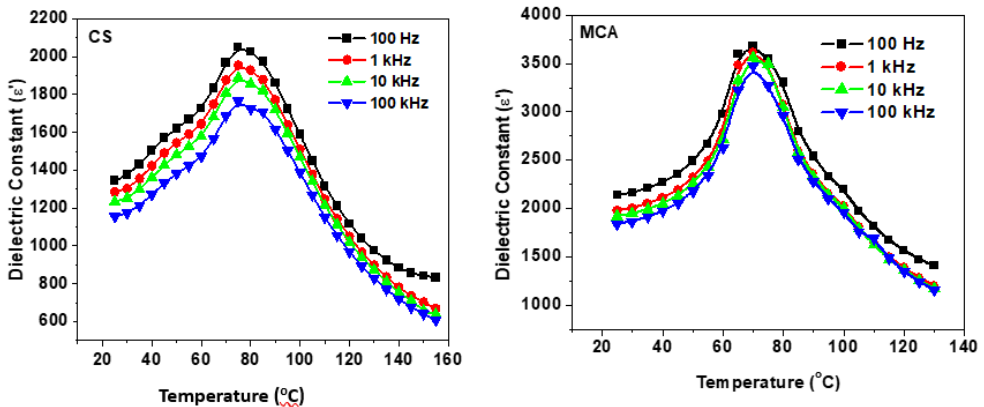


Fig. 4. Dielectric constant versus temperature

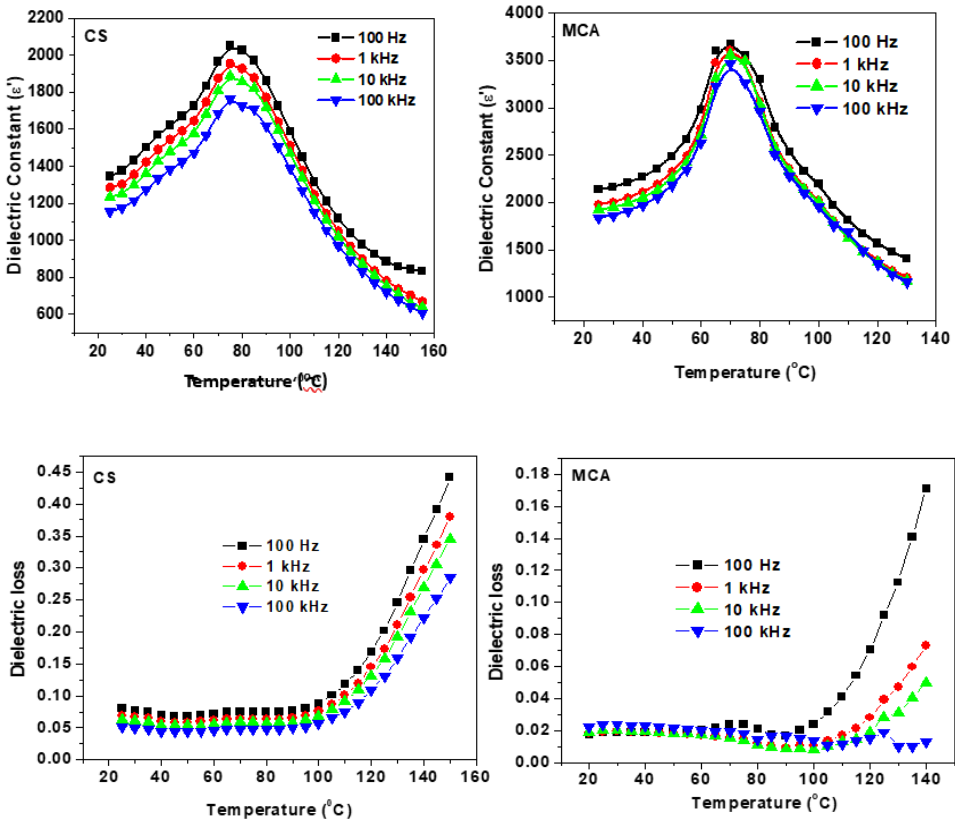


Fig. 5. Dielectric loss versus temperature

3.3 Ferroelectric Properties

Figure 6 shows the hysteresis loops (P-E loop) at ambient conditions of BTW ceramic at 1 Hz and 20 kV/cm. The P-E loop of ball milling and mechanical activation method shown in the figure exhibits ferroelectric behavior. Loops exhibit higher values of both residual polarization (P_r) and coercive field (E_c) for ball milling compared to the activation process loop of BTW but exhibit lower values compared to the typical ferroelectric loop. The lower values of P_r and E_c may be attributed towards the enhanced domain pinning the residual vacancies as larger grains have larger remanent polarization [21-23].

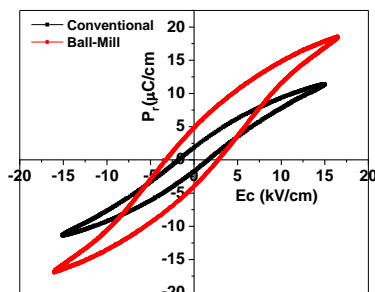


Fig. 6. P-E Loops of BTW

4 Conclusion

The BTW was prepared by two different methods i.e., conventional ball milling and mechanical activation process to compare the structural and dielectric properties. The XRD confirms the tetragonal structure for both methods with the same values of crystallite size, lattice parameters, and cell volume. Further, the SEM and TEM reveal that the particles size milled for 30 hours reduces to nano-range. The curie temperature comes around 70-80oC for both the methods and loss tangent shows a bit different variation as the loss tangent for both the methods seen saturated initially, then, there is a rapid increase in the higher temperature range for ball milling whereas not much increase in case of mechanical activation method. The P-E loop exhibits the low value of P_r and E_c with a higher saturation value for the solid-state compared to the mechanical activation process. Hence the samples made by both methods demonstrate comparable properties.

References

- [1] F. Jona, G. Shirane, *Ferroelectric crystals*, Dover Publications, INC, New York, chapter V11, (1962)
- [2] Wu, Menghao, *Nature Reviews Physics* 3.11: 726-726 (2021)
- [3] L.L. Hench, J. K. West, *Principles of Electronics Ceramics*, Wiley & Sons, New York, p. 202 (1990)
- [4] M. Waqar, H. Wu, J. Chen, K. Yao, J. Wang, *Advanced Materials* **34** (2021)
- [5] F. Wan, J. han, Z. Zhu, *Phys. Lett. A* 372, 2137-2140 (2008)
- [6] J.Z. Jiang, F.W. Poulsen, S. Mørup, *Journal of Materials Research* 14 1343–1352 (1999)
- [7] J.Z. Jiang, R. Lin, W. Lin, K. Nielsen, S. Mørup, K. Dam-Johansen, R. Clasen, *Journal of Physics D: Applied Physics* **30** 1459–1467 (1997)
- [8] M. Simoneau, G. L'Espérance, M.L. Trudeau, R. Schulz, *Journal of Materials Research* **9** 535–540 (1994)
- [9] D.J. Fatemi, V.G. Harris, V.M. Browning, J.P. Kirkland, *Journal of Applied Physics* **83** 6867–6869 (1998)
- [10] S. Devi, P. Ganguly, S. Jain, A.K. Jha, *Ferroelectrics* **381** 120–129 (2009)
- [11] S. Devi and A. K. Jha, *Physica B* **404**, 4290–4294 (2009)
- [12] S. Devi and A. K. Jha, *Current Applied Physics* **11** S95-S99 (2011)

- [13] S. Chaudhary, M. Chaudhary, S. Devi, S. Jindal, *Journal of Theoretical and Applied Physics*, **17**(2) (2023).
- [14] V. Kavitha, P. Mahalingam, M. Jeyanthinath, N. Sethupathi, *Materials Today: Proceedings* **23** 12–15 (2020)
- [15] W.R. BUESSEM, L.E. CROSS, A.K. GOSWAMI, *Journal of the American Ceramic Society* **49** 33–36 (1966)
- [16] G. Arlt, D. Hennings, G. de With, *Journal of Applied Physics* **58** 1619–1625 (1985)
- [17] W. Känzig, *Physical Review* **98** 549–550 (1955)
- [18] K. Uchino, E. Sadanaga, T. Hirose, *Journal of the American Ceramic Society* **72** 1555–1558 (1989)
- [19] R. Jasrotia, V.P. Singh, B. Sharma, A. Verma, P. Puri, R. Sharma, M. Singh, *Journal of Alloys and Compounds* **830** 154687 (2020)
- [20] W.D. Callister Jr, *Anti-Corrosion Methods and Materials* **47** (2006)
- [21] T. Friessnegg, S. Aggarwal, R. Ramesh, B. Nielsen, E.H. Poindexter, D.J. Keeble, *Applied Physics Letters* **77** 127–129 (2000)
- [22] R. Jasrotia, P. Puri, V.P. Singh, R. Kumar, *Journal of Sol-Gel Science and Technology* **97** 205–212 (2020)
- [23] S.K.S. Parashar, R.N.P. Choudhary, B.S. Murty, *Journal of Applied Physics* **94** 6091–6096 (2003)
- [24] R. KODURI, M. LOPEZ, *Ferroelectrics Letters Section* **34** 113–123 (2007)